

Effects of small amount Ta on the characteristics of the Zr-Al-Ni-Cu-Ta bulk metallic glass

Hongchao Kou¹), Xidong Hui¹), Xiongjun Liu¹), Xiping Song¹), Guoliang Chen¹), and Kefu Yao²)

1) State Key Laboratory for Advanced Metals and Materials, University of Science and Technology Beijing, Beijing 100083, China

2) Mechanical Department, Tsinghua University, Beijing 100081, China

(Received 2004-02-20)

Abstract: The effects of Ta on the characteristics of the Zr-base BMG (bulk metallic glass) were investigated. $Zr_{55}Al_{10}Ni_5Cu_{30-x}Ta_x$ ($x=1, 2, 4$) bulk metallic glasses (BMGs) with 3.5 mm diameter and 70 mm length were successfully prepared by using combined jet and copper mold casting. A small amount of Ta addition does not change the glass transition temperature, crystallization temperature, and supercooled liquid region obviously, but Ta promotes composition separation and two-stage crystallization. The stable crystalline phases include Zr_2Ni , $CuZr_2$, Al_2Zr_3 intermetallic compounds and Ta-rich solid solution after annealing the Zr-Al-Ni-Cu-Ta alloys at 753 K. $Zr_{55}Al_{10}Ni_5Cu_{30-x}Ta_x$ ($x=1, 2, 4$) bulk glassy alloys exhibit a better compressive strength. The stress-strain curve shows a zig-zag feature, and the fracture surface shows intersecting of shear bands. It may correlate with the inhomogeneous feature of amorphous structure.

Key words: Zr-Al-Ni-Cu-Ta alloy; bulk metallic glass (BMG); microstructure; compressive property

[This work was financially supported by the National Natural Science Foundation of China (No.50171005 and 50171006), the National Hi-tech Research and Development Program of China (No.2001AA331010), the National Major Basic Research Project of China (No.G2000 67201-3) and the Major Science and Technology Program of Beijing (No.H020420030320).]

1 Introduction

Zr-base bulk metallic glasses (BMGs) have been investigated comprehensively because of their excellent glass forming ability and workability in the supercooled liquid region, which makes it easy to fabricate bulk glassy samples and complex-shaped components as novel structural engineering materials [1-2]. However, the brittle fracture features and catastrophic failure at room temperature because of localized shear deformation seriously limit the application of BMGs. Zr-Al-Ni-Cu quaternary BMGs have been studied by adding W, Ta to significantly improve the strength and ductility due to the formation of in-situ nano or micrometer ductile phase or particles [3-5]. For example, $(Zr_{70}Ni_{10}Cu_{20})_{90-x}Ta_xAl_{10}$ ($0 \leq x \leq 12$) alloys form two-phase microstructures consisting of crystalline Ta-rich solid solution particles embedded in BMG matrix [6], Ta also promotes the formation of bcc- β -Zr (Ta, Cu, Ni, Al) dendrites and induces the precipitation of Zr_2Cu and Zr_2Ni intermetallics for the $Zr_{66.4}Cu_{10.5}Ni_{8.7}Al_8Ta_{6.4}$ alloy [7], which lead the alloys to show much a larger plastic strain or higher yield

strength. In this work, $Zr_{55}Al_{10}Ni_5Cu_{30-x}Ta_x$ ($x=1, 2, 4$) bulk metallic glass formation alloys are prepared by using copper mold casting and the effects of small amount Ta on the characteristics of Zr-Al-Ni-Cu-Ta BMG, regarding their as-cast microstructure, thermal stability, and compressive behavior, are also investigated.

2 Experimental procedure

The BMG forming alloys with a nominal composition of $Zr_{55}Al_{10}Ni_5Cu_{30-x}Ta_x$ ($x=1, 2, 4$) were prepared by arc melting the pure metals (99.9wt% or better in purity) in a Ti-gettered argon atmosphere in order to obtain the master alloy, followed by induction melting the master alloy and injection casting into a water-cooling copper mold to form 70 mm-long cylinders with 3.5 mm in diameter. Due to the very high melting temperature of Ta, master alloy ingots were prepared by two-step process: the element zirconium and tantalum were melted together to produce a homogeneous ingot; then the nickel, copper and aluminum were melted together with the zirconium-tantalum alloy ingot, the ingots were melted and flipped several times

to promote homogeneity in each step. The processing can make sure that Ta completely dissolves into the melt. The cylindrical samples were cut to 2 mm thick and annealed for 10 min at near the crystallization temperature under argon atmosphere to investigate the thermal stability of the alloys.

Cross sections of cast rods were examined by X-ray diffraction (XRD) using Cu- K_{α} radiation. The glass transformation and crystallization of the samples was studied with a differential scanning calorimeter (Netzsch DSC 204) at a heating rate of 0.33 K/s. The microstructure was examined by JEM 2000FX transmission electron microscopy (TEM) and JEM 2010FEF high-resolution TEM operated at 200 kV. Compression tests were performed on a Gleeble 1500 thermal simulate testing machine at a constant strain rate of 10^{-4} s^{-1} at room temperature. The compression specimens were cut to a length that provided an aspect ratio of 2.0. The ends of the rods were ground flat and perpendicular to the loading axis. After the mechanical tests, SEM was used to investigate the fracture surface.

3 Results and discussion

The X-ray diffraction patterns for the as-cast $\text{Zr}_{55}\text{Al}_{10}\text{Ni}_5\text{Cu}_{30-x}\text{Ta}_x$ ($x=1,2,4$) alloys are shown in **figure 1**. The diffraction patterns show a broad scattering feature at $2\theta=33\text{-}43^\circ$ and no appreciable sharp Bragg peaks corresponding to crystalline phases. The broad scattering feature is characteristic of an amorphous phase. Therefore the X-ray diffraction proves that the alloys are full amorphous alloys. No diffraction peaks of Ta or other crystalline phases are detected within the sensitivity limit of XRD until Ta content reaches 4at%.

The structures of as-cast cylindrical samples of $\text{Zr}_{55}\text{Al}_{10}\text{Ni}_5\text{Cu}_{30-x}\text{Ta}_x$ ($x=2$ and 4) alloys were also observed by TEM and high-resolution TEM. The elec-

tron diffraction patterns, shown in **figure 2** (a) and (b) for $\text{Zr}_{55}\text{Al}_{10}\text{Ni}_5\text{Cu}_{30-x}\text{Ta}_x$ with $x=2$ and 4 respectively, also prove amorphous structures without obvious crystalline diffraction spots. However, the TEM image shows an inhomogeneous feature that may be a reflection of composition separation. The area of the separation regions is about 20-50 nm. The alloy with 4at% Ta ($x=4$) exhibits a stronger feature of the composition separation than the alloy with 2at% Ta ($x=2$). The reference [8] indicated that Ta has a significant effect on the average near-neighbor atomic environment. Figure 2(c) shows the HRTEM image for $\text{Zr}_{55}\text{Al}_{10}\text{Ni}_5\text{Cu}_{30-x}\text{Ta}_x$ ($x=4$). It can be easily found that is an amorphous structure, and no grain boundary and no crystalline lattice can be seen. If the HRTEM image is carefully examined, however, abound short-range order (SRO) with <1-2 nm in size can be found. Our previous work [9] has proved that the SRO structures in $\text{Zr}_{52.5}\text{Cu}_{17.9}\text{Ni}_{14.6}\text{Al}_{10}\text{Ti}_5$ BMGs are similar to the fcc and tetragonal Zr_2Ni structure. It is not clear that the relationship between composition separation and the SRO structure. Now, the investigation on this problem is conducting.

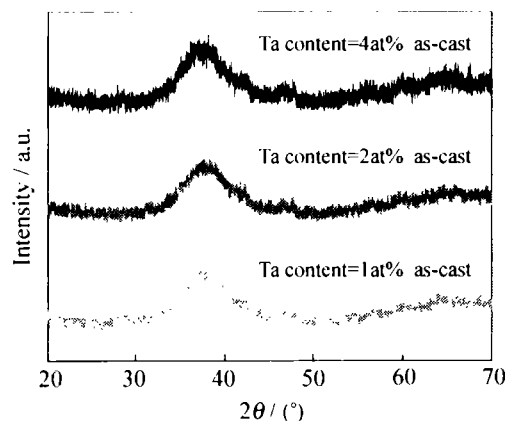


Figure 1 XRD patterns for the as-cast bulk $\text{Zr}_{55}\text{Al}_{10}\text{Ni}_5\text{Cu}_{30-x}\text{Ta}_x$ ($x=1,2,4$) metallic glasses.

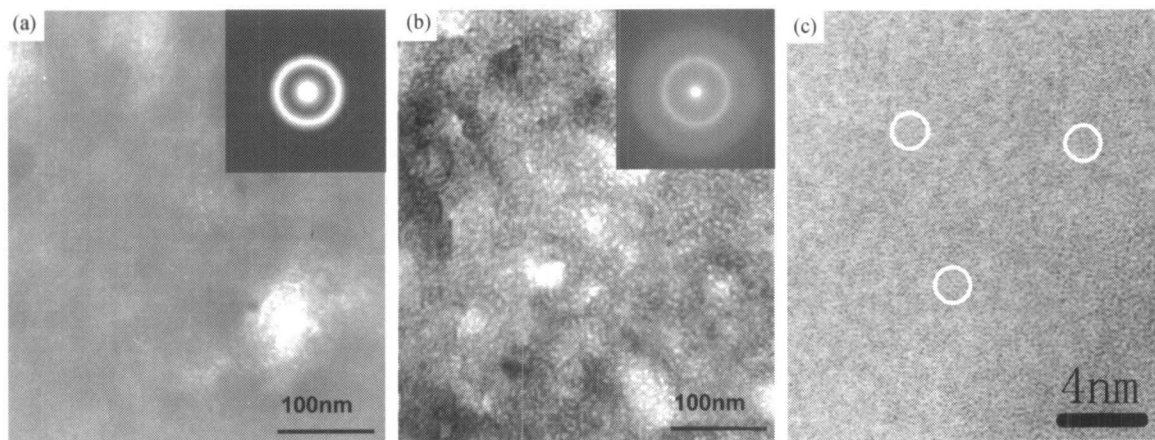


Figure 2 Bright-field TEM, HRTEM images and selected-area diffraction of the as-cast microstructure for $\text{Zr}_{55}\text{Al}_{10}\text{Ni}_5\text{Cu}_{30-x}\text{Ta}_x$ ($x=2,4$) bulk metallic glasses: (a) and (b) are TEM images for $\text{Zr}_{55}\text{Al}_{10}\text{Ni}_5\text{Cu}_{30-x}\text{Ta}_x$ ($x=2,4$) respectively, (c) is HRTEM image for $\text{Zr}_{55}\text{Al}_{10}\text{Ni}_5\text{Cu}_{26}\text{Ta}_4$.

DSC curves for the cylindrical $Zr_{55}Al_{10}Ni_5Cu_{30-x}Ta_x$ ($x=1,2,4$) alloys are shown in **figure 3**. The DSC curve for the 1at% Ta alloy shows a single exothermic peak, which is the same as the $Zr_{55}Al_{10}Ni_5Cu_{30}$ alloy [10]. For the 2at% and 4at% Ta alloys, the second exothermic peak begins to appear at near 850 K. These two alloys exhibit two-stage exothermic reaction characteristics. The values of T_g (glass transition temperature), T_x (crystallization temperature), T_{p1} (the first peak temperature) and ΔT_x (supercooled liquid region) are listed in **table 1**. It can be seen that the Ta addition do not change obviously the values of T_g , T_x , and ΔT_x in the $Zr_{55}Al_{10}Ni_5Cu_{30}$ BMG alloy.

It has been reported that the addition of Ta element in Zr-base BMGs promotes to formed β -Zr(Ta). Ott RT and his coworkers have reported that the alloy with 8at% Ta can lead to precipitate bcc Ta-rich solid solute particles even during solidification in $(Zr_{70}Cu_{20}Ni_{10})_{90-x}Ta_xAl_{10}$ system [6]. At the same time, the 5at% Ta addition leads to the increase in the T_g and decrease the ΔT_x [11]. However in the present study,

no β -Zr(Ta) solid solution was obtained for the as-cast 3.5 mm cylinders of the alloy with 4at% Ta. Moreover, the values of T_g , T_x and ΔT_x remain almost unchanged.

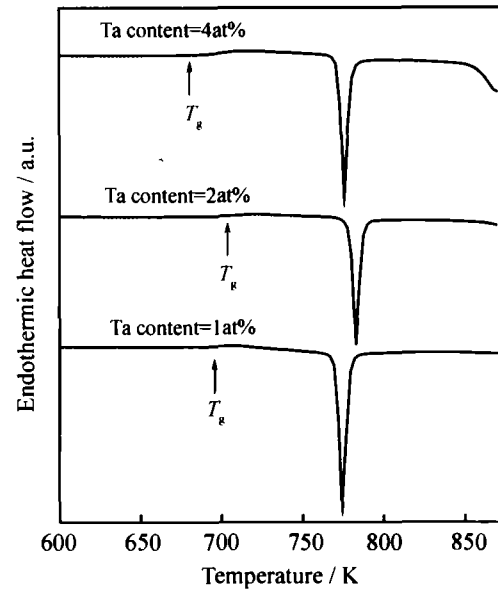


Figure 3 DSC traces of $Zr_{55}Al_{10}Ni_5Cu_{30-x}Ta_x$ ($x=1,2,4$) bulk metallic glasses.

Table 1 T_g , T_x , T_{p1} , and ΔT_x of $Zr_{55}Al_{10}Ni_5Cu_{30-x}Ta_x$ bulk metallic glasses

x	$T_{g, onset} / K$	$T_{g, offset} / K$	T_x / K	T_{p1} / K	$\Delta T_x / K$
0*	680	—	755	767	83
1	696	697	768	775	72
2	703	712	777	784	74
4	689	705	771	776	82

Note: $T_{g, onset}$ is the onset temperature of glass transition, $T_{g, offset}$ is the offset temperature of glass transition;

* this data is cited from reference [10].

By annealing the samples of $Zr_{55}Al_{10}Ni_5Cu_{30-x}Ta_x$ ($x=2,4$) at 753 K for 10 min, we examined the effect of small amount of Ta addition on the thermal stability of Zr-base BMGs. The XRD patterns are shown in **figure 4**. It can be seen that heating the as-cast cylinders to near T_x leads to the formation of Zr_2Ni , $CuZr_2$, Al_2Zr_3 intermetallic compounds and the precipitation of β -Zr(Ta) solid solution.

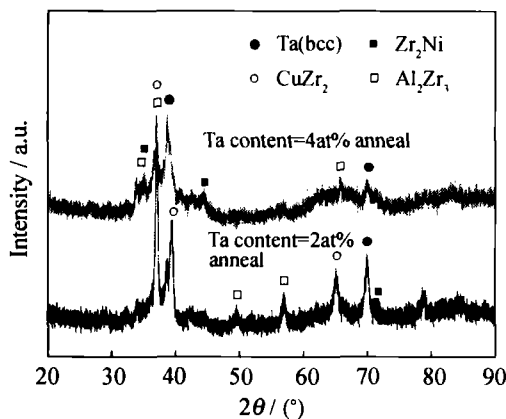


Figure 4 XRD patterns for the annealing $Zr_{55}Al_{10}Ni_5Cu_{30-x}Ta_x$ ($x=1,2,4$) alloys at 753 K for 10 min.

Figure 5 shows the results of compressive tests of $Zr_{55}Al_{10}Ni_5Cu_{30-x}Ta_x$ ($x=1,2,4$) bulk glassy alloys with 3.5 mm in diameter. The compressive fracture strength, fracture strain and Young's modulus are 1761 MPa, 1.96 and 93 GPa for the 1at% Ta alloy and 1893 MPa, 2.13 and 90 GPa for the 4at% Ta alloy, respectively. By comparison with common Zr-base BMGs, the addition of Ta shows significantly strengthening effects at the same time without loss in fracture strain. It should emphasize that the stress-strain curves exhibit a zig-zag feature.

Figure 6 shows the fracture morphology of the as-cast $Zr_{55}Al_{10}Ni_5Cu_{26}Ta_4$ BMG. The final fracture takes place along the maximum shear plane, which is decline by about 45° to the direction of compressive loading. The fracture surface morphology of the as-cast $Zr_{55}Al_{10}Ni_5Cu_{26}Ta_4$ exhibits a well-developed vein pattern, as shown in **figure 6(a)**. However, as the magnification of the picture is increased (as insert part in **figures 6 (b) and (c)**), we can see the more complex fracture surface. The intersecting of different shear

bands indicates an inhomogeneous deformation in the different areas of the fracture surface. It may be a kind of inhomogeneous deformation or 'localized deformation bands', which may correlate with the zig-zag feature in the loading curve. The shear bands also can adjust their space by branching, as shown in figure 6(d), which is observed on the side surface of the testing specimen.

The two-stage crystallization, zig-zag loading curve and intersecting of different fracture feature of as-cast $Zr_{55}Al_{10}Ni_5Cu_{30-x}Ta_x$ ($x=1,2,4$) bulk glassy alloys may fully be related with the composition separation. As increasing the Ta content from 1at% to 4at% the inhomogeneous microstructure as well as the intersecting of shear deformation becomes more obvious, which has significance on the strength of the alloy.

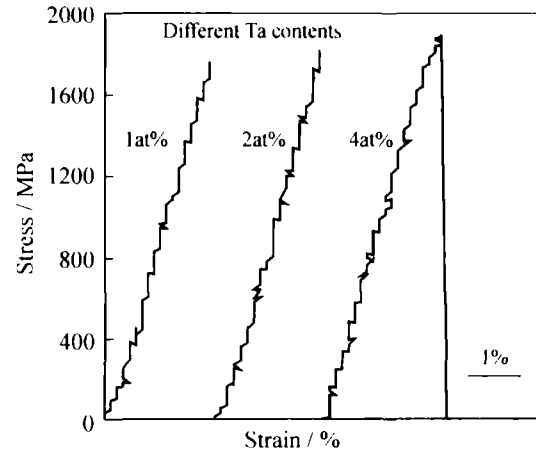


Figure 5 Room temperature compressive stress-strain curves of $Zr_{55}Al_{10}Ni_5Cu_{30-x}Ta_x$ ($x=2,4$) cylinder BMGs.

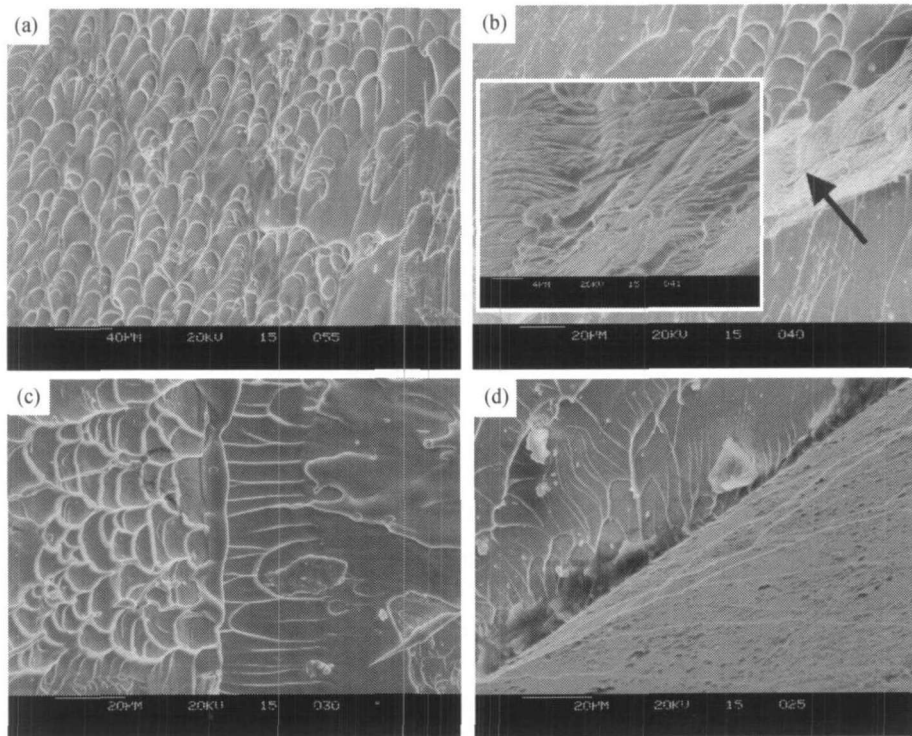


Figure 6 Fracture surface of as-cast $Zr_{55}Al_{10}Ni_5Cu_{26}Ta_4$ BMG with 3.5 mm in diameter: (a) the typical vein pattern of the fracture surface; (b) and (c) show the more complex fracture surface, the insert in (b) is magnification of area marked with the black arrow; (d) an area of the fracture surface which has experienced shear band branching during fracture.

4 Conclusions

(1) $Zr_{55}Al_{10}Ni_5Cu_{30-x}Ta_x$ ($x=1,2,4$) bulk metallic glasses with 3.5 mm in diameter and 70 mm in length were successfully prepared by using combined jet and copper mold casting.

(2) A small amount of Ta addition does not change the values of T_g , T_x , and ΔT_x obviously in Zr-base BMGs. But Ta promotes composition separation and two-stage crystallization. The stable crystalline phases include Zr_2Ni , $CuZr_2$, Al_2Zr_3 intermetallic compounds and Ta-rich solid solution after annealing the Zr-Al-

Ni-Cu-Ta alloys at 753 K.

(3) $Zr_{55}Al_{10}Ni_5Cu_{30-x}Ta_x$ ($x=1,2,4$) bulk metallic glasses exhibit a better compressive strength. The stress-strain curve shows a zig-zag feature, and the fracture surface shows intersecting of shear bands. It may correlate with the inhomogeneous feature of amorphous structure.

References

- [1] A. Inoue, *Bulk Amorphous Alloys*, Trans Tech Publication LTD, Switzerland, 2000.
- [2] W.L. Johnson, Bulk amorphous metal—An emerging en-

- gineering material, *JOM*, 3(2002), p.40.
- [3] H. Choi-Yim, R. Busch, U. Köster, *et al.*, Synthesis and characterization of particulate reinforced $Zr_{57}Nb_5Al_{10}Cu_{15.4}Ni_{12.6}$ bulk metallic glass composites, *Acta Mater.*, 47(1999), No.8, p.2455.
- [4] J. Saida, A. Inoue, Icosahedral quasicrystalline phase formation in Zr–Al–Ni–Cu glassy alloys by the addition of V, Nb and Ta, *J. Non-Cryst. Solids*, 312-314(2002), p.501.
- [5] X.D. Hui, H.C. Kou, J.P. He, *et al.*, Preparation, microstructure and mechanical properties of Zr-based bulk amorphous alloys containing tungsten, *Intermetallics*, 10(2002), p.1065.
- [6] R.T. Ott, C. Fan, J. Li, *et al.*, Structure and properties of Zr–Ta–Cu–Ni–Al bulk metallic glasses and metallic glass matrix composites, *J. Non-Cryst. Solids*, 317(2003), p. 158.
- [7] G. He, W. Löser, J. Eckert, Microstructure and mechanical properties of the $Zr_{66.4}Cu_{10.5}Ni_{8.7}Al_8Ta_{6.4}$ metallic glass-forming alloy, *Scripta Mater.*, 48(2003), p.1531.
- [8] T.C. Huftnagel, C. Fan, R.T. Ott, *et al.*, Controlling shear band behavior in metallic glasses through microstructural design, *Intermetallics*, 10(2002), p.1163.
- [9] G.L. Chen, X.D. Hui, S.W. Fan, *et al.*, Concept of multi-component chemical short range order (MCSRO) and glass forming ability, *Intermetallics*, 10(2002), p.1221.
- [10] L. Liu, Z.F. Wu, J. Zhang, Crystallization kinetics of $Zr_{55}Cu_{30}Al_{10}Ni_5$ bulk amorphous alloy, *J. Alloys Compd.*, 339(2002), p.90.
- [11] G. He, W. Löser, J. Eckert, *et al.*, Phase transformation and mechanical properties of Zr-base bulk glass-forming alloys, *Mater Sci. Eng.*, A352(2003), p.179.